

# Dielectrophoretic Microfluidic Chip Enables Single-Cell Measurements for Multidrug Resistance in Heterogeneous Acute Myeloid Leukemia Patient Samples

Avid Khamenehfar,<sup>†</sup> Maher K. Gandhi,<sup>#</sup> Yuchun Chen,<sup>†</sup> Donna E. Hogge,<sup>||</sup> and Paul C. H. Li<sup>\*,†,⊥</sup>

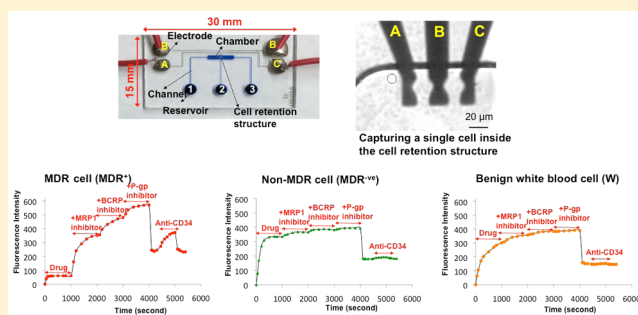
<sup>†</sup>Department of Chemistry, <sup>⊥</sup>Department of Molecular Biology and Biochemistry, Simon Fraser University, 8888 University Drive, Burnaby, British Columbia, Canada

<sup>#</sup>The University of Queensland, Diamantina Institute, 37 Kent Street, Woolloongabba, Queensland, Australia

<sup>||</sup>Terry Fox Laboratory, BC Cancer Agency, 675 West 10th Avenue, Vancouver, British Columbia, Canada

## Supporting Information

**ABSTRACT:** The front-line treatment for adult acute myeloid leukemia (AML) is anthracycline-based combination chemotherapy. However, treatment outcomes remain suboptimal with relapses frequently observed. Among the mechanisms of treatment failure is multidrug resistance (MDR) mediated by the ABCB1, ABCC1, and ABCG2 drug-efflux transporters. Although genetic and phenotypic heterogeneity between leukemic blast cells is a well-recognized phenomenon, there remains minimal data on differences in MDR activity at the individual cell level. Specifically, functional assays that can distinguish the variability in MDR activity between individual leukemic blasts are lacking. Here, we outline a new dielectrophoretic (DEP) chip-based assay. This assay permits measurement of drug accumulation in single cells, termed same-single-cell analysis in the accumulation mode (SASCA-A). Initially, the assay was optimized in pretherapy samples from 20 adults with AML whose leukemic blasts had MDR activity against the anthracycline daunorubicin (DNR) tested using multiple MDR inhibitors. Parameters tested were initial drug accumulation, time to achieve signal saturation, fold-increase of DNR accumulation with MDR inhibition, ease of cell trapping, and ease of maintaining the trapped cells stationary. This enabled categorization into leukemic blast cells with MDR activity (MDR<sup>+</sup>) and leukemic blast cells without MDR activity (MDR<sup>-ve</sup>). Leukemic blasts could also be distinguished from benign white blood cells (notably these also lacked MDR activity). MDR<sup>-ve</sup> blasts were observed to be enriched in samples taken from patients who went on to enter complete remission (CR), whereas MDR<sup>+</sup> blasts were frequently observed in patients who failed to achieve CR following front-line chemotherapy. However, pronounced variability in functional MDR activity between leukemic blasts was observed, with MDR<sup>+</sup> cells not infrequently seen in some patients that went on to achieve CR. Next, we tested MDR activity in two paired AML patient samples. Pretherapy samples taken from patients that achieved CR to front-line chemotherapy were compared with samples taken at time of subsequent relapse. MDR<sup>+</sup> cells were frequently observed in leukemic blast cells in both pretherapy and relapsed samples, consistent with MDR as a mechanism of relapse in these patients. We demonstrate the ability of a new DEP microfluidic chip-based assay to identify heterogeneity in MDR activity in leukemic blasts. The test provides a platform for future studies to characterize the mechanistic basis for heterogeneity in MDR activity at the individual cell level.



Acute myeloid leukemia (AML) is a cancer of abnormally differentiated clonal myeloid precursor cells (leukemic blasts) present in the bone marrow and peripheral blood.<sup>1</sup> Front-line treatment consists of multiagent combination chemotherapy incorporating anthracyclines such as daunorubicin (DNR). Nearly 80% of patients with AML achieve initial remission after combination chemotherapy,<sup>2,3</sup> but subsequently, many relapse and become insensitive to further treatment.<sup>4</sup> Unfortunately, the majority of relapsed patients eventually die of their disease, with only ~10% of patients surviving.<sup>5,6</sup>

A major limitation to the success of combination chemotherapy in AML is the resistance of leukemia blast cells to a spectrum of anticancer drugs that are mechanistically and structurally unrelated, a phenomenon known as multidrug resistance (MDR).<sup>7,8</sup> A well-established cause of MDR involves the increased efflux of hydrophobic cytotoxic drugs mediated by ATP binding cassette (ABC) transporters. These ABC transporters, or MDR proteins, principally include ABCB1

Received: November 24, 2015

Accepted: May 5, 2016

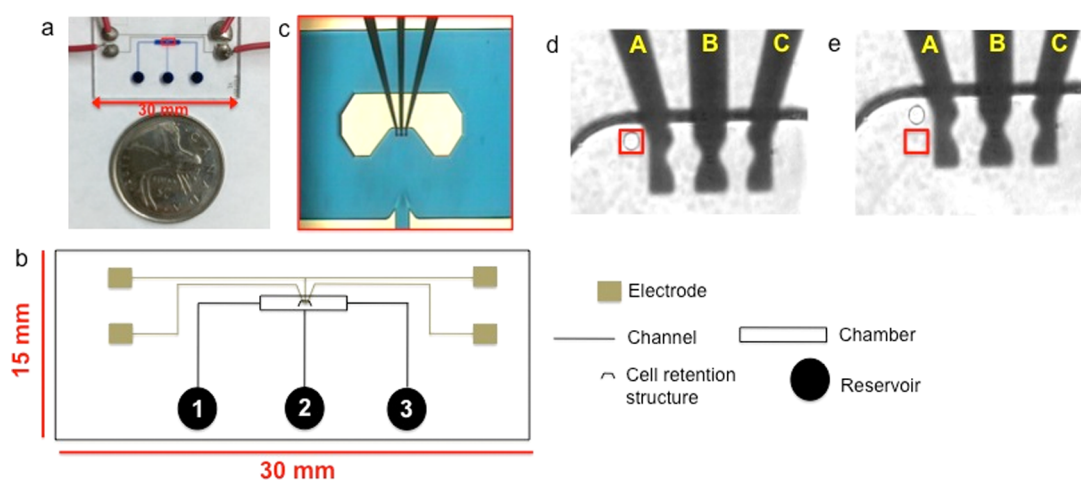


**Figure 1.** Microfluidic chip with DEP electrodes located in the cell retention structure. (a) Image of the microchip with channels filled with a blue food dye for easy visualization and with electrodes connected to electrical wires. A quarter (25 cents) coin was placed next to the chip for size comparison. (b) Layout of the microfluidic DEP chip, with the left and right reservoirs serving as the cell inlet and waste reservoirs, respectively; whereas the middle reservoir is used for drug delivery. (c) The close-up of the chamber with cell retention structure and DEP electrodes. (d, e) Image of a cell captured and retained near electrode A. The cell was selected by microfluidic flow into the cell retention structure and retained by the DEP force near the left side of electrode A. The chip is translated to shuttle the cell down (d) and up (e) into the detection window (red box) to measure the cellular signal and background, respectively. An alternating electric field of 11.5 V at 3 MHz was applied to keep the cell close to electrode A during SASCA-A experiment.

(also known as P-glycoprotein or P-gp), ABCC1 (also multidrug resistance-associated protein 1 or MRP1), and ABCG2 (also breast cancer resistance protein or BCRP).<sup>9,10</sup> The increased expression of these transporters causes active transport of chemotherapeutic drugs out of leukemic blasts, reducing the amount of accumulated drug and impacting the effectiveness of chemotherapy.<sup>11–13</sup> Approximately 50% of AML patients have leukemic blasts that express ABC transporters, with increased levels of expression in elderly and relapsed patients.<sup>8,14,15</sup> Furthermore, AML leukemic blasts frequently express more than one type of MDR proteins, especially at relapse.<sup>16</sup>

Inhibition of ABC transporters to reverse MDR is a potential adjuvant to chemotherapy. However, clinical trials evaluating the strategy of inhibiting efflux-mediated chemotherapeutic resistance have been disappointing,<sup>17</sup> and so elucidation of MDR mechanisms to enable the rational design of novel approaches remains a priority.<sup>18,19</sup> Conventionally, the MDR function was studied by measuring drug accumulation using a variety of methods including flow cytometry,<sup>20</sup> radiolabeling-based microtiter plate assays.<sup>21</sup> However, these methods are “bulk assays”, and experiments require a substantial number of cells which are not always available. Moreover, biological heterogeneity is notably recognized in the mechanisms that underpin MDR within leukemic blasts,<sup>12</sup> but a particular limitation of existing “bulk assays” is that heterogeneity at the individual leukemic blast cell level obscures the results of drug accumulation measurements. Moreover, the experiments are technically demanding and time-consuming, involving multiple steps such as drug incubation followed by cell washing, and cell lysis to release drug content for radioactive measurement. In addition, the use of ionizing radiation in radioactive measurements introduces safety concerns.

In order to study the MDR function at the single-cell level, we previously used a microfluidic chip to conduct same-single-cell analysis in the drug accumulation mode (SASCA-A).<sup>22–25</sup> However, this chip cannot easily retain patient cells, and so we designed a new dielectrophoretic (DEP) chip for the functional

assay. Assay of drug accumulation was performed in the absence of MDR inhibitor and then in the presence of a MDR inhibitor to permit the same leukemic blast cell to serve as its own internal control. The method also provides time-dependent drug transport data on a single cell and permits morphological interrogation, which allows us to categorize different single cells.

## EXPERIMENTAL SECTION

**Microchip.** As shown in Figure 1a,b, the dielectrophoretic (DEP) microchip (15 mm × 30 mm) consists of three channels, three reservoirs, and one chamber containing the cell retention structure to trap the single cell. What is new is the inclusion of embedded electrodes in the retention structure to conduct DEP-based cell trapping. The microfluidic chip was fabricated using the standard micromachining procedures on glass by CMC Microsystems (Kingston, ON, CA). These procedures include standard chip cleaning, thin metal film deposition, photolithography, photoresist development, glass etching by hydrofluoric acid, reservoir forming on cover plate, and chip bonding.<sup>26–28</sup>

Reservoirs 1 and 3 served as the inlet and waste reservoirs, respectively, whereas reservoir 2 was used for drug delivery. The channel was 40 μm deep, while the reservoirs (2.5 mm in diameter) were 0.6 mm deep. Three DEP electrodes (platinum 180 nm/tantalum 20 nm) have been embedded in the cell retention structure (Figure 1c). As shown in Figure 1d,e, a single AML cell was captured in the retention structure near the DEP electrodes, and the cell was in the same location during drug accumulation measurement, while the chip was translated up and down.

**Dielectrophoresis To Retain an AML Single Cell.** Since leukemic blast cells are in suspension and would be flushed away during the switch of reagents in experiments, an advanced method is required to trap a single cell and keep it stationary during fluorescent measurement. Dielectrophoresis (DEP) has been used to manipulate polarizable microparticles,<sup>29</sup> such as cells, which are suspended in a liquid medium. While the DEP

technique was previously used to sort cells,<sup>30</sup> or trap them,<sup>31</sup> this method has not been used to shuttle the cells between two positions. We tried to use DEP electrodes to shuttle single cells by electrode polarity switching. Although we managed to move the single cell back and forth, we could not bring the cell back to the same location precisely. Therefore, we used this DEP technique in a different way such that the cell was kept stationary, while the chip was shuttled for measurement of drug accumulation in the cell.

Our results showed that the cancerous cells were easily retained near electrode A (see Figure 1d) for experiments. It was important to optimize the frequency and magnitude of the alternating electric voltage applied to the electrodes to retain the cell but not to damage it by high voltage. In order to trap a single leukemic blast cell and keep it in the same location for all experiments, different voltages (5, 7, 9, 10, 11, 11.5, 13 V) as well as frequencies (1, 2, 3, 5 MHz) were tested. As for the nonleukemic blasts one issue is that they are hard to be captured by DEP, as they did not remain stationary during SASCA-A experiments. This observation was consistent with previous reports that DEP was able to isolate leukemic blast cells from nonleukemic blast cells, such as white blood cells (WBCs), that are of similar sizes.<sup>32,33</sup> To overcome the nonstationary issue, the WBCs were kept within the cell retention structure by controlling the liquid flow manually during the entire experiment.

**Reagents.** Daunorubicin (DNR), cyclosporine A (CsA), MK571, and fumitremorgin C (FTC) were purchased from Sigma-Aldrich (St Louis, MO). Iscove's modified Delbecco medium (IMDM) and fetal bovine serum (FBS) were obtained from Life Technologies (Grand Island, NY). Hanks' balanced salt solution (HBSS) was purchased from Invitrogen Corp (Grand Island, NY). DNR was dissolved in dimethyl sulfoxide (DMSO, Sigma-Aldrich) to make stock solutions of 350  $\mu$ M. Similarly, stock solutions of MK571 (1 mM), CsA (500  $\mu$ M), FTC (1 mM), and  $\text{NaN}_3$  (1 mM) were made in DMSO. Alexa Fluor 488-labeled antihuman CD34 monoclonal antibody was purchased from Biologend (San Diego, CA) and it was diluted in HBSS (1:20 ratio) before use.<sup>34,35</sup>

**AML Patient Cell Samples.** The AML patient cells were obtained from cryopreserved peripheral blood samples. The cells were thawed and mixed in 10 mL of IMDM with 20% FBS and spun at 1000 rpm for 10 min. This was followed by resuspending the cells in 1 mL of IMDM plus 5% FBS. All experiments on patient cells were performed within 48 h after thawing.

In the initial cohort, 20 samples of cryopreserved AML patient cells were provided by the BC Cancer Agency after receiving research ethical approval (BCCA-REB H10-03343). Table S1 lists their clinical characteristics (see Supporting Information). Samples were taken pretherapy, that is, prior to administration of combination chemotherapy. The clinical designation of these patients to chemotherapy was either refractory or complete remission (CR). CR is defined as a reduction of leukemic blasts within the bone marrow to a morphologically undetectable level (leukemic blast count of  $\leq 5\%$ ) with normal peripheral blood cell counts.<sup>36</sup> However, a substantial burden of leukemia cells can remain undetected, leading to later relapse. No information existed on outcome as to whether patients entering CR subsequently relapsed.

In order to conduct studies on patient samples at relapse, we utilized a second cohort, that is, paired peripheral blood samples from two patients provided by the Australian Leukemia

and Lymphoma Group (ALLG) Tissue Bank after receiving research ethical approval (ALLG Tissue Bank TB035). The samples for each patient were collected pretherapy and at relapse occurring 5–6 months later. Table S2 illustrates the information provided by ALLG Tissue Bank for the two patient samples (see Supporting Information).

**On-Chip Drug Accumulation Measurement on the AML Single Cells.** Single cells were selected by size and morphological criteria for SASCA-A measurements using the microfluidic chip. Briefly, after the cells were introduced from the inlet reservoir (reservoir 1 in Figure 1a), solutions from two other reservoirs were removed. Once the liquid pressure difference was established, the cells flowed from left to right inside the cell chamber toward the retention structure. By adjusting the liquid levels of reservoirs 1 and 3, the cell moved back to the entrance of the cell retention structure, and then the cell was pushed into the structure by a flow induced via reservoir 2 (Figure 1b).

To trap the cell and keep it at the same location for all experiments, DEP<sup>37,38</sup> was used with the assistance of applying appropriate AC voltage between electrodes A and B.<sup>39</sup> An AC voltage of 11.5 V (3 MHz) was used to keep the AML cell stationary. The trapped cell (Figure 1d,e) was settled for  $\sim 10$  min before fluorescence measurements commenced.

An optical detection system was employed for simultaneous fluorescence measurement and bright-field imaging. In SASCA-A, the first step was to measure the accumulation of DNR in the AML leukemic blast (by measuring levels of single-cell fluorescence) in the absence of MDR inhibitors.<sup>22–24</sup> The inherent fluorescence of DNR is  $\lambda_{\text{ex}} = 470$  nm;  $\lambda_{\text{em}} = 585$  nm.<sup>22–24</sup> Thereafter, drug accumulation was measured in the same single cell in the presence of MDR inhibitor compounds (MK571, CsA or FTC). During SASCA-A measurement, the chip was moved down and up across the detection aperture window (depicted by the red box in Figure 1d,e) to detect the cell signal and the background, respectively. When the cell was inside the detection window, the cellular fluorescence was measured; whereas the background was measured when the cell was outside the detection window. Subtraction of the background from the cell signal gave a corrected signal representing the drug concentration in the cell.<sup>22–24</sup> After performing the experiments, the cell trapped inside the retention structure was washed with HBSS (2 $\times$ ), and then Alexa Fluor 488 antihuman CD34 antibody (diluted in HBSS in a ratio of 1:20) was added to recognize CD34<sup>+</sup> AML blasts. After all experiments, the cell was treated with trypan blue to test cell viability. Trypan blue is a small molecule (2–10 nm),<sup>40</sup> and is therefore able to penetrate into nonviable cells through pores formed by toxins (such as DNR) to stain the cell blue.

**Flow Cytometry.** Bulk drug accumulation measurement in cells was performed by a flow cytometer (Guava easyCyte 8HT, EMD Millipore, Billerica, MA). Briefly, an aliquot (1 mL) of the cell suspension ( $\sim 300000$  cells/mL) was mixed with 10 mL of IMDM with 20% FBS and spun down. Then, 1 mL of cell medium (IMDM with 5% FBS) with DNR was mixed with the cell pellet and the mixture was transferred to a plastic tube. Drug accumulation in cells was conducted at 24  $^{\circ}\text{C}$  for 30 min in the dark. After centrifugation (1000 rpm for 5 min) and removal of the supernatant, the cells were reincubated in the medium alone (i.e., without DNR) for an additional 30 min (to start drug efflux). After a second centrifugation (1000 rpm for 5 min), the supernatant was removed. Cold HBSS (4  $^{\circ}\text{C}$ ) was then added to each tube to quench the efflux. This procedure

was repeated for the MDR reversal study with the first incubation with DNR and then a second incubation of the cell medium with an inhibitor (i.e., MK571 or CsA).

The cell suspensions (control and inhibitor-treated) were transferred to a microwell plate for flow cytometry analysis. Fluorescence intensity ( $\lambda_{\text{ex}} = 470 \text{ nm}$ ,  $\lambda_{\text{em}} = 585 \text{ nm}$ ) was collected and displayed. The time needed to complete the procedure of incubation, centrifugation, reincubation, and analysis was  $\sim 140 \text{ min}$ , as previously noted.<sup>27</sup>

## RESULTS AND DISCUSSION

**Categorization of Leukemic Blast Cells in Patient Samples.** Since the activity of more than one type of MDR transporters has been reported in the cancer cells of AML patients, the drug accumulation experiments were evaluated on AML single cells using different categories of MDR inhibitors, specifically MK571 (a MRP1 inhibitor), FTC (a BCRP inhibitor), and CsA (a P-gp inhibitor). Initially, MK571 and CsA were tested on the MDR reversal effect of DNR accumulation. The optimal concentrations for DNR, MK571, and CsA have been obtained as described in Supporting Information.

Figure 2 shows the SASCA-A experiment on three single cells obtained from a refractory sample (patient sample 1 or p-AML 1). As illustrated in Figure 2a, the initial fluorescence signal of

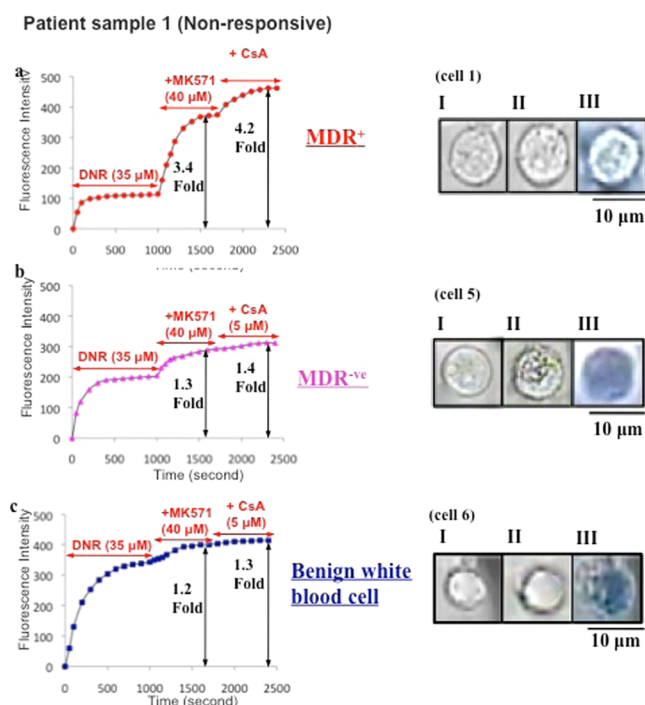


**Figure 2.** DNR accumulation in AML patient single cells after treating them with MDR inhibitors. The cells were obtained from an AML patient (p-AML 1), who was clinically refractory;  $40 \mu\text{M}$  of MK571 and  $5 \mu\text{M}$  of CsA were used as the MDR inhibitors. (a) In cell 1, the MDR inhibitors enhanced DNR accumulation in the single cell. (b) Cell 5 shows a high initial signal (in counts per second) and no significant drug enhancement after adding MDR inhibitors. (c) The single cell 6 did not show any drug enhancement after treating with MDR inhibitors. The size of cell 6 was smaller as compared to the other two cells. The cell images of cells 1, 5, and 6, respectively, were depicted (I) before experiment, (II) after experiment, and (III) followed by trypan blue treatment. Scale bar:  $10 \mu\text{m}$ .

the DNR was low ( $110 \pm 39 \text{ cps}$ ) after cell 1 (from p-AML 1) was administered with DNR ( $35 \mu\text{M}$ ). After  $40 \mu\text{M}$  of MK571 and  $5 \mu\text{M}$  of CsA were added, the signals were enhanced to  $375 \pm 43$  and  $460 \pm 45 \text{ cps}$  (fold-increases of 3.4 and 4.2), respectively. This cell was indicative of MDR since the initial drug accumulation was low and its value was enhanced by the coadministration of MDR inhibitors. The cell was categorized as  $\text{MDR}^+$ .

For cell 5 (Figure 2b) the initial fluorescence signal was not low ( $195 \pm 51 \text{ cps}$ ), and the time to gain steady state was shorter (300 s to reach saturation) than for cell 1 (100 s to reach saturation). Moreover, the fluorescence signal only slightly increased after coadministering DNR and MK571 or CsA ( $1.3 \pm 0.2$  or  $1.5 \pm 0.2$  of fold-increases, respectively). Since the drug efflux process due to MDR transporters plays an important role in the rate of attaining steady state in drug accumulation, the slow rate of drug accumulation for cell 5 results in its categorization as non-MDR or its designation as  $\text{MDR}^{-\text{ve}}$ .

The morphologies of these two single cells are shown before and after experiment using bright-field imaging and after trypan blue exclusion assay to confirm cell viability. As shown in Figure 2, cell 5 was stained positive (Figure 2bIII) and cell 1 was stained negative (Figure 2aIII), consistent with cytotoxicity in an  $\text{MDR}^+$  leukemic blast being more difficult to achieve.

Cell 6, shown in Figure 2c, had features distinct from cell 1, but similar to cell 5. As with cell 5, the initial fluorescence signal of cell 6 was high ( $340 \pm 56 \text{ cps}$ ) and there was no obvious drug enhancement observed after coadministration of MDR inhibitors (folds of  $1.2 \pm 0.2$  and  $1.3 \pm 0.2$  with MK571 and CsA, respectively). However, the drug accumulation in cell 6 took a longer time than cell 5 to reach plateau, 840 s for cell 6 but 300 s for cell 5.

The bright-field imaging during experiments also allowed direct observation of cells after they were captured by DEP at the chip surface. Whereas cells 1 and 5 remained stationary during the experiment, cell 6 was hard to retain by DEP and the cell was kept within the cell retention structure only by continuously adjusting the liquid flow, that is, from left or right of the retention structure. Moreover, cell 6 would be distinguishable by size because it had a smaller size than cells 1 and 5, see cell images I for the three cells in Figure 2. These findings are consistent (although not definitive) with cell 6 being a benign white blood cell (termed W). Benign white blood cells should not overexpress ABC drug transporters (thus, DNR would take longer to reach saturation or plateau) nor should there be drug enhancement after treatments by ABCB1 or ABCC1 inhibitors.

In remaining experiments, the cells were categorized to be  $\text{MDR}^+$ ,  $\text{MDR}^{-\text{ve}}$  and W, which was based on initial signal (by adding DNR alone), fold-increase with the use of MDR inhibitors (MK571 and CsA), trypan blue exclusion, ease of DEP capture, and the stationary nature of the cell during experiments. Table S3 summarizes the categorization of the three types of single cells found in the same patient samples.

**Behavior of Cells in Refractory Patient Samples.** Other than pAML1, the remaining refractory samples were tested by SASCA-A.  $\text{MDR}^+$  cells (low initial fluorescent intensities and high fold increases) formed the majority of cells in 8 of 10 refractory patients. As shown in Figure 3, 24 of 36 cells examined were  $\text{MDR}^+$  cells. Among the remaining 12 cells, 5 benign white blood cells were found in p-AML 1 (cell 6), p-AML 10 (cell 18), p-AML12 (cell 24), p-AML 15 (cell 30), and

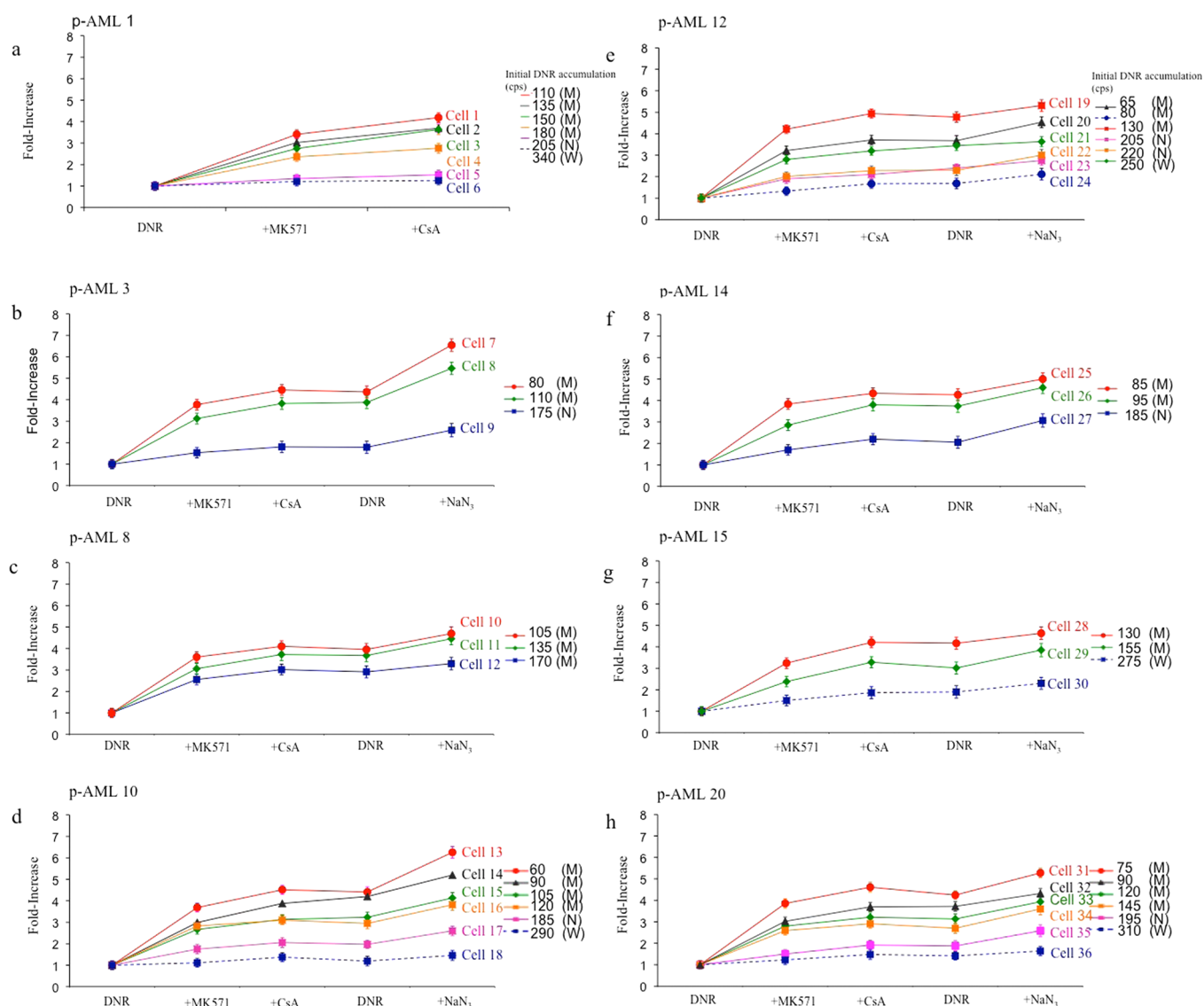


**Figure 3.** MDR<sup>+</sup> (M) cells found in refractory AML patient samples. The reagents used were DNR (35  $\mu$ M), MK571 (40  $\mu$ M), CsA (5  $\mu$ M), and NaN<sub>3</sub> (1 mM). (a–h) Fold-increases in DNR accumulation in single cells obtained from AML patients 1, 3, 8, 10, 12, 14, 15, and 20, respectively. The number on the legend represents the initial fluorescent intensity (in counts per second). Dashed lines represented single cells that were nonstationary, which was the characteristics of benign cells (W). Solid lines represented cells that were stationary, which were the characteristics of both MDR<sup>+</sup> (M) and MDR<sup>ve</sup> (N) cells. The raw data for single cells 1, 5, and 6 were shown in Figure 2.

p-AML 20 (cell 36), while the remaining seven cells were MDR<sup>ve</sup> cells. In most experiments, we observed that when the inhibitor was removed, no signal attained due to DNR was lost, suggesting that MDR inhibition had persisted and DNR was still effectively retained within the cell. Thereafter, the single cells were further treated with sodium azide (NaN<sub>3</sub>, 1 mM) to inhibit ATPase in the cell and block the function of the energy-dependent ABC transporters (taken as 100% inhibition).<sup>41</sup> The ratio between the fluorescence signal of the MDR inhibitor-blocked and that of the NaN<sub>3</sub>-blocked cells could indicate the extent of MDR reversal of the inhibitor.

In two refractory patient samples (p-AML 9 and p-AML 16, Figure S2), MDR<sup>ve</sup> cells (high initial counts and low fold-increases) were unexpectedly more abundant than MDR<sup>+</sup> cells. Although only a limited number of single cells were tested, here as with other experiments, heterogeneity at the single-cell level in MDR inhibitor responsiveness was again demonstrable. To confirm that these were leukemic blasts but not benign white

blood cells, flow cytometry was performed on bulk (300,000) cells for p-AML 9 (Figure S4c), confirming that the cells were blasts and they were generally refractory to the MDR inhibitor MK571 (no right shift of the DNR+MK571 peak from the DNR-only peak in Figure S4c). This implicates non-ABCB1 transporter mechanisms may have mediated DNR resistance in this patient. Moreover, nonpump resistance mechanisms might be involved and they include drug inactivation, degradation, antiapoptotic, and antioxidant defenses, as well as DNA repair.<sup>42,43</sup>

**Effect of MDR Inhibitors on Complete Remission (CR) Patient Samples.** Experiments were performed on single cells obtained from 10 CR samples (see Figures 4 and S3). Given the limited numbers of patient samples and single cells tested, and the unavailability of information on subsequent relapse in patients attaining CR, no comparison between patients in different clinical categories was made. However, it was evident that single-cell heterogeneity was prominent in the CR samples,

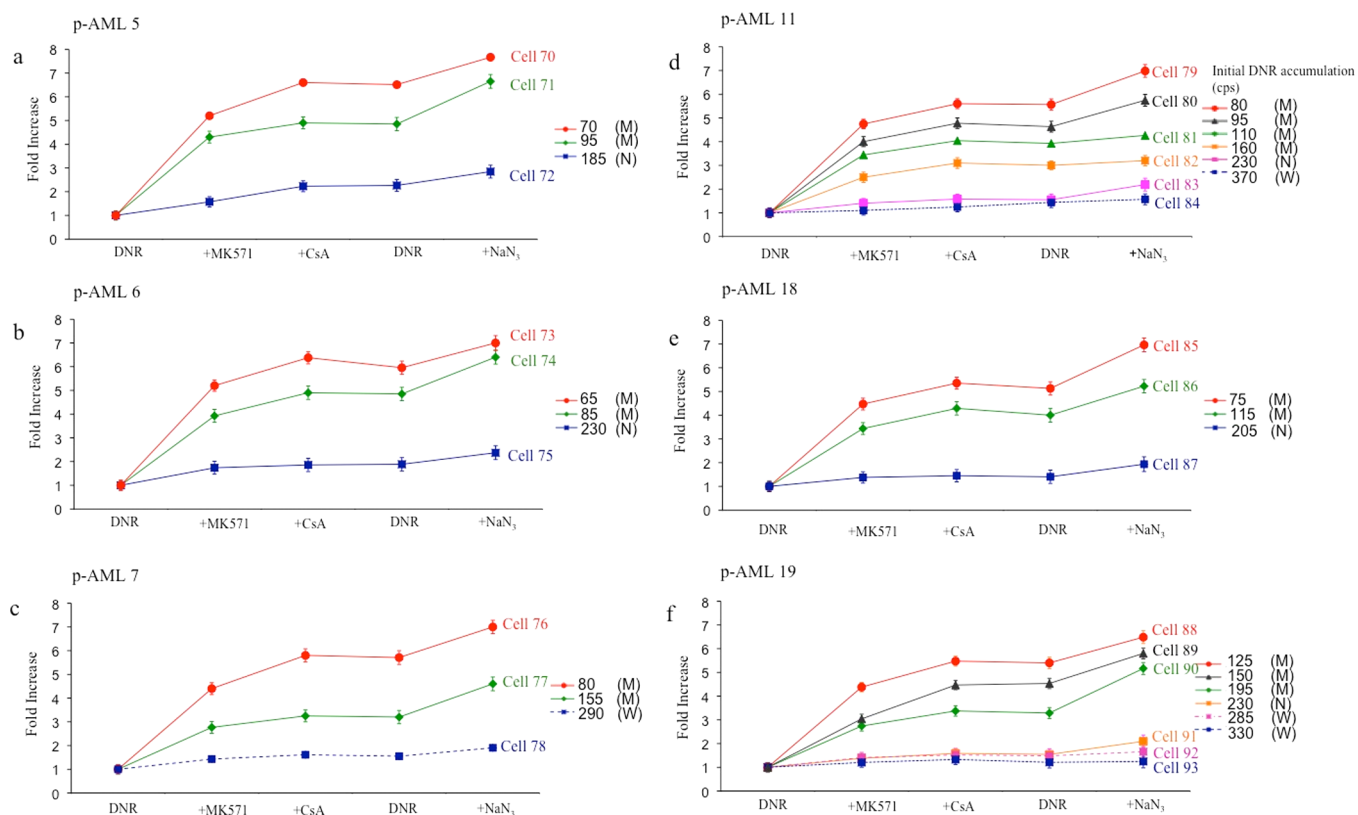


**Figure 4.** MDR<sup>+</sup> (M) cells also found in complete remission (CR) AML patient samples. (a–f) Fold-increase of DNR accumulation in cells obtained from patients 5, 6, 7, 11, 18, and 19. The number on the legend represents the initial fluorescent intensity. Dashed lines represented cells that were nonstationary, which was the characteristics of benign cells (W). Solid lines represented cells that were stationary which were the characteristics of both MDR<sup>+</sup> (M) and MDR<sup>-ve</sup> (N) cells. The MDR<sup>+</sup> cells in CR samples were surprisingly found to have greater fold-increases (5–7-fold) than the MDR<sup>+</sup> cells in refractory samples (3–4-fold).

with not only MDR<sup>-ve</sup> cells, but also MDR<sup>+</sup> cells identified (Figure 4), and with cells 78, 84, 92, and 93 categorized as benign. Interestingly, marked variability in fold-increases was observed in MDR<sup>+</sup> leukemic blast cells across CR and refractory samples (Figures 3 and 4).

#### Effect of Multiple MDR Inhibitors on Single Cells Collected from AML Patient Samples Pretherapy and at Relapse.

Subsequent experiments were performed to measure the MDR reversal effect on AML cell samples from two patients (p-AML 21 and p-AML 22), in whom blood was collected pretherapy and at relapse. p-AML 21 had a higher blast count (92 and 97% of blasts in peripheral blood pretherapy and at relapse, respectively) compared to p-AML 22 (63 and 67%, respectively). Six single cells were selected from the pretherapy sample of p-AML 21, all successfully captured by DEP near electrode A (see Figure 1) and easily kept stationary during the experiment. Only one cell represented the characteristics of the MDR<sup>+</sup> cell. As shown in Figure 5d, the drug accumulation rate in cell 104 after adding DNR alone was fast (i.e., saturation attained at a short time of ~58 s). This indicated the strong drug efflux due to the increased expression of MDR in the captured single cell. Thereafter, the signal reached a plateau as the drug uptake rate was close to the drug efflux rate. In the cell, the addition of multiple MDR inhibitors (40  $\mu$ M of MK571, 20  $\mu$ M of FTC, and 5  $\mu$ M of CsA) caused the single-cell fluorescence to increase by 2.1-, 2.7-, and 3.0-fold, respectively. After washing the cell with HBSS (2 $\times$ ), the fluorescence signal dropped. Addition of the anti-CD34 antibody increased the fluorescent signal from 185 to 283

cps, confirming the captured cell was a leukemic blast expressing CD34. Five other single cells from the same pretherapy sample were individually captured and examined based on the similar cell selection process for cancerous cells. Figure 5a–c,e,f, but not Figure 5d, show that the initial DNR signals were high and no significant fold-increase was observed after adding MDR inhibitors (MK571, FTC, and CsA). Moreover, cells 101, 102, 103, 105, and 106, but not cell 104, took up trypan blue (see cell images III).

Similar experiments were performed on single cells obtained from the relapse sample of the same patient (p-AML 21). These cells were easily captured near electrode A after applying the DEP force, and they remained stationary during experiments. As shown in Figure 6a–d notable enhancement in fluorescent intensity was observed in the four cells due to the administration of three MDR inhibitors (fold-increases of 3.5, 4.7, 5.8 in cell 107; 4.9, 6.5, 7.7 in cell 108; 4.5, 5.8, 6.6 in cell 109, and 4.6, 5.0, 5.2 in cell 110). These high fold-increases are characteristics of MDR<sup>+</sup> cells. In this limited number of tested cells, the fold-increases were higher as compared to the values obtained for the cells in the pretherapy sample of the same patient. The four cells were also CD34<sup>+</sup> and excluded trypan blue (Image III in Figure 6a–d). Cell 112 had features of a benign white blood cell. First, it was difficult to be trapped by DEP and it required flow control to keep the cell within the cell retention structure during the experiment. Second, it depicted high initial DNR signal and no significant fold-increase after adding MDR inhibitors (Figure 6f). Unlike the other examined cells, the accumulation rate in cell 112 was slow and the signal

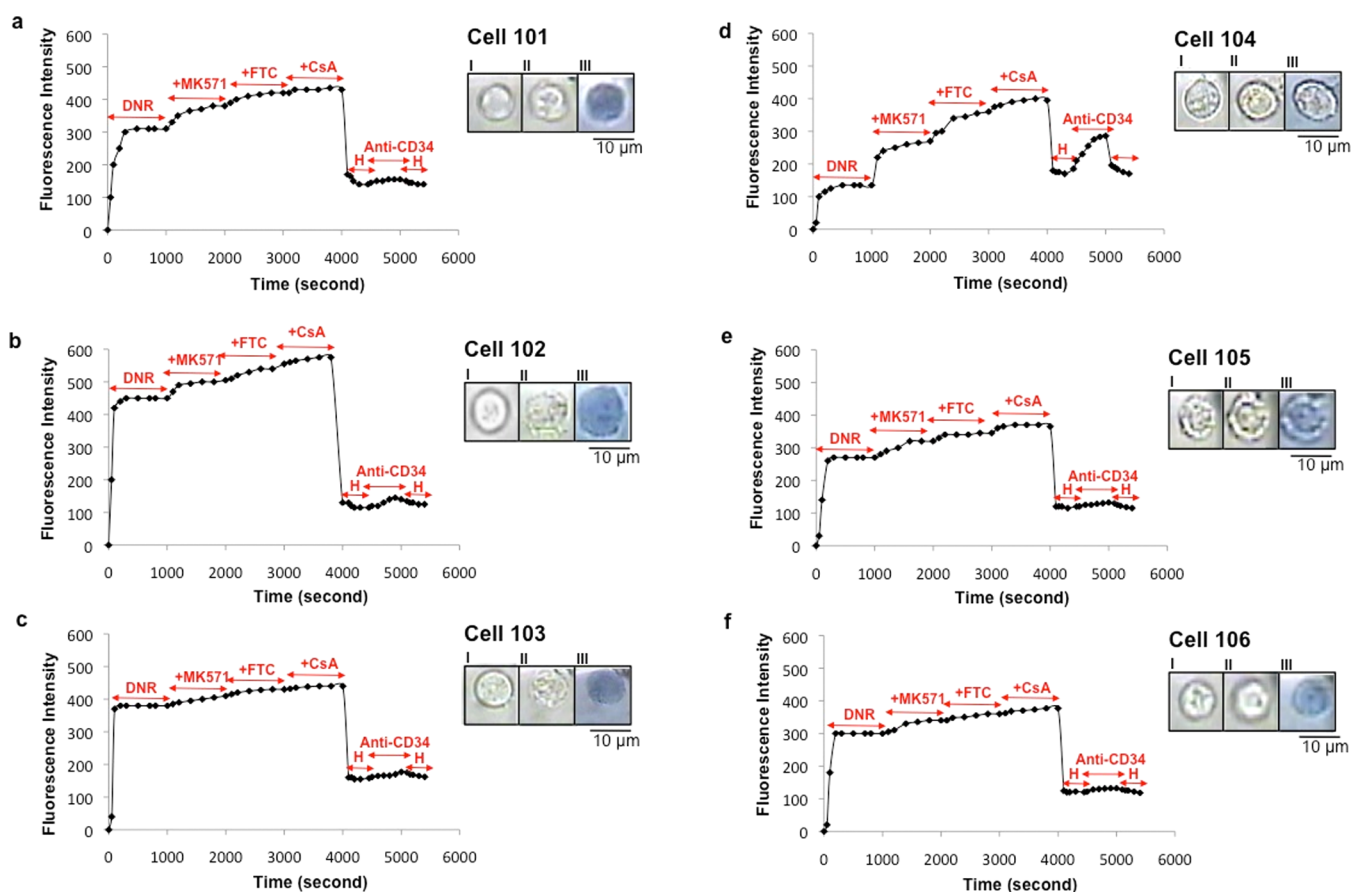


**Figure 5.** Fluorescent measurement of single cells obtained from the AML pretherapy sample. The patient single cells were treated with drug + MDR inhibitors (40  $\mu$ M of MK571, 20  $\mu$ M of FTC, and 5  $\mu$ M of CsA). The fluorescent emission wavelength was changed from 585 nm (to measure DNR) to 524 nm (to measure anti-CD34) at 4000 s. Only in cell 104, the MDR inhibitors (i.e., MK571, FTC, and CsA) enhanced DNR accumulation. The rest of five other examined single cells did not show any significant drug accumulation enhancement. The images of cells 101–106 were depicted (I) before experiment, (II) after experiment, and (III) followed by adding trypan blue. Only cell 104 was not stained, and the fluorescence signal of this cell alone increased after adding anti-CD34 antibody. Scale bar: 10  $\mu$ m.

reached a plateau at a long time of  $\sim$ 780 s, and it was stained by trypan blue.

For another patient (i.e., p-AML 22), even though the blast count was low, there was no trouble in finding MDR<sup>+</sup> and MDR<sup>-ve</sup> single cells, which were big in cell size, for experiments, see Figure S5. Similar results of DNR accumulation was found, with both MDR<sup>+</sup> and MDR<sup>-ve</sup> single cells observed in pretherapy sample (four out of six single cells were MDR<sup>-ve</sup>, Figure S6) and five out of six examined single cells (cells 119–123) at relapse classified as MDR<sup>+</sup> (Figure S7). A benign white blood cell is depicted in Figure S7f.

## CONCLUSIONS

We used a newly designed dielectrophoretic (DEP) biochip with the same-single-cell analysis in the accumulation mode (SASCA-A) to test for single-cell heterogeneity in multidrug resistance (MDR)-based drug efflux function. The assay was optimized in samples from patients with acute myeloid leukemia (AML). The microfluidic DEP chip was successfully used to trap single leukemic blasts that were categorized as MDR<sup>+</sup> and MDR<sup>-ve</sup> and to distinguish these from benign white blood cells. However, pronounced variability in MDR in leukemic blasts was observed at the single-cell level, with MDR<sup>+</sup> single cells found in complete remission (CR) samples.

Initially, the SASCA-A assay was optimized in pretherapy samples from 20 adults with AML and the cells had MDR activity against daunorubicin (DNR) when tested using multiple MDR inhibitors. Parameters tested were initial drug accumulation, rate to achieve signal saturation, fold-increase of DNR accumulation due to MDR inhibition, ease of cell trapping, and the ease of maintaining the trapped cells stationary, as summarized in Table S3. Using coadministration of MDR inhibitors of ABCB1, ABCC1, and ABCG2, pronounced variability in functional MDR activity between leukemic blasts was observed. Next, we tested MDR activity in samples taken pretherapy in two patients that achieved CR to front-line chemotherapy and compared them with paired samples taken at time of subsequent relapse. MDR was frequently observed in leukemic blast cells in both pretherapy and relapsed samples, consistent with MDR as a mechanism of relapse in these patients.

MDR is a recognized factor for relatively high failure rate of anthracycline-based combination chemotherapy in AML. Biological heterogeneity within leukemic blasts is also well established.<sup>12</sup> The limited number of patient samples and cells examined prevent any clinical inferences to be made. Rather, we demonstrate that this method can be a useful tool to investigate the heterogeneity of MDR inhibition at the single-cell level in AML leukemic blasts. This novel assay provides a platform that can be used for future studies to characterize the

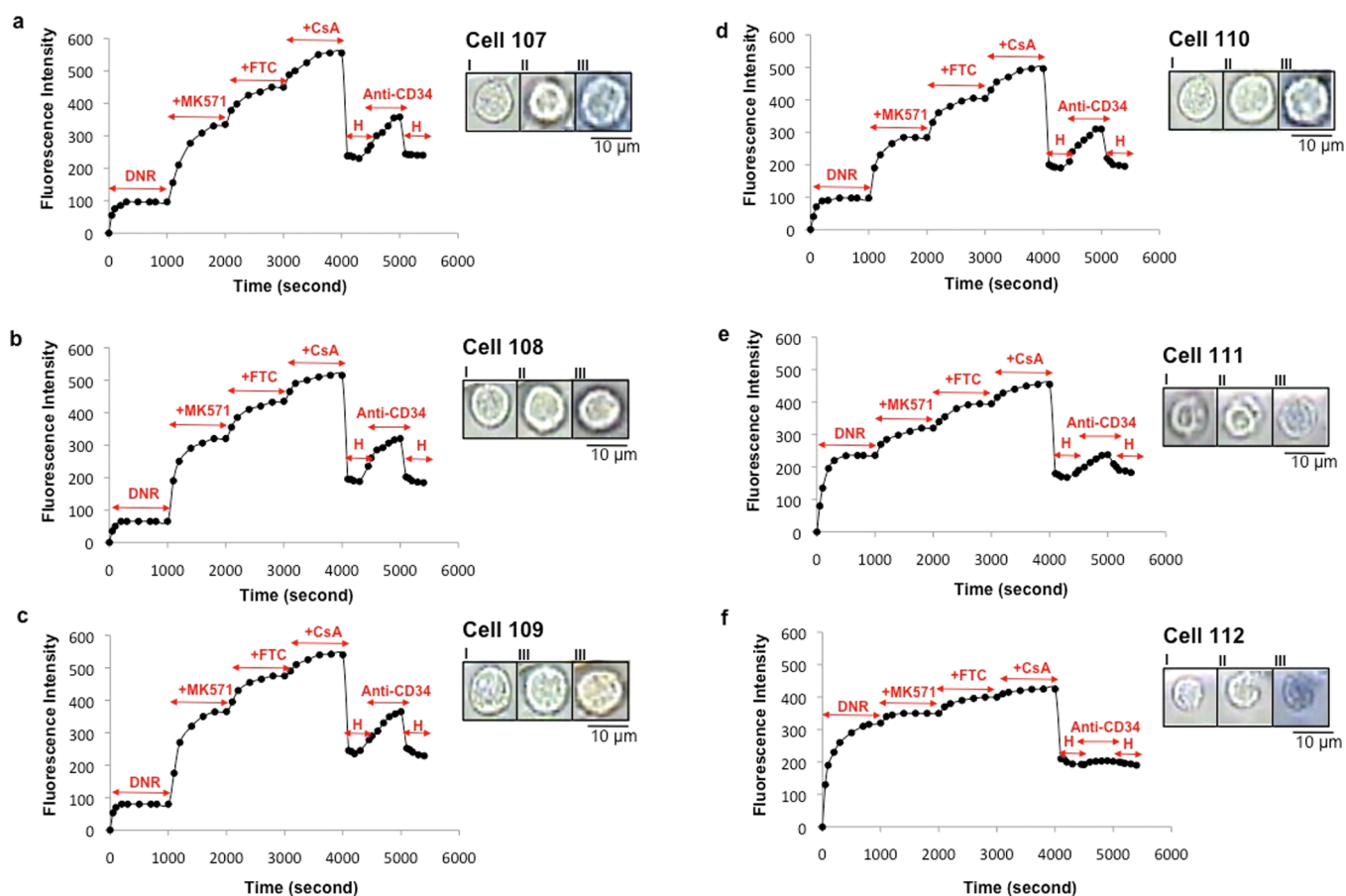


**Figure 6.** Fluorescent measurement of single cells obtained from the AML relapse sample. (a, c, e, g, i, k) The patient single cells were treated with drug + MDR inhibitors (40  $\mu$ M of MK571, 20  $\mu$ M of FTC, and 5  $\mu$ M of CsA), followed by addition of anti-CD34 antibody. Cells 107–111 indicated significant drug accumulation enhancement and they expressed CD34. Only in cell 112, there was no enhancement in drug accumulation due to MDR inhibitors, and the cell did not express CD34. The images of cells 107–112, respectively, were depicted (I) before experiment, (II) after experiment, and (III) followed by adding trypan blue. Only cell 112 was stained. Scale bar: 10  $\mu$ m.

mechanistic basis for heterogeneity in MDR activity at the individual malignant cell level in AML and in other cancer types.

## ■ ASSOCIATED CONTENT

### Supporting Information

The Supporting Information is available free of charge on the ACS Publications website at DOI: 10.1021/acs.analchem.5b04446.

Additional experimental details and supporting figures (PDF).

## ■ AUTHOR INFORMATION

### Corresponding Author

\*Tel.: (778) 782-5956. Fax: (778) 782-3765. E-mail: paulli@sfu.ca.

### Notes

The authors declare no competing financial interest.

## ■ ACKNOWLEDGMENTS

Financial support from Natural Science and Engineering Research Council (NSERC) is acknowledged. We also thank BC Cancer Agency and ALLG Tissue Bank, which have provided the cryopreserved patient samples.

## ■ NOMENCLATURE

ABCB1 ATP-binding cassette subfamily B member 1; ABCB1 ATP-binding cassette subfamily C member 1; ABCG2 ATP-binding cassette subfamily G member 2; AML acute myeloid leukemia; BCRP breast cancer resistant protein; CD34 haematopoietic progenitor cell antigen-1; CsA cyclosporine A; CR complete remission; DEP dielectrophoresis; DMSO dimethyl sulfoxide; DNR daunorubicin; FBS fetal bovine serum; FTC fumitremorgin C; HBSS Hanks' balanced salt solution; IMDM Iscove's modified Delbecco medium; MDR multidrug resistance; MRP1 multidrug resistance protein 1; SASCA-A same-single-cell analysis in the drug accumulation mode; p-AML patient with acute myeloid leukemia; PEN/STR penicillin/streptomycin; P-gp permeability glycoprotein

## ■ REFERENCES

- (1) Dohner, H.; Weisdorf, D. J.; Bloomfield, C. D. *N. Engl. J. Med.* **2015**, *373*, 1136–52.
- (2) Jiang, X. J.; Kai-Kai, H.; Mo, Y. *Cancer Lett.* **2012**, *326* (2), 135–142.
- (3) O'Donnell, M. R.; Abboud, C. N.; Altman, J.; et al. *J. Natl. Compr. Canc. Netw.* **2012**, *10* (8), 984–1021.
- (4) Tallman, M. S.; Gilliland, D. G.; Rowe, J. M. *Blood* **2005**, *106*, 1154–1163.
- (5) Breems, D. A.; Van Putten, W. L.; Huijgens, P. C.; et al. *J. Clin. Oncol.* **2005**, *23*, 1969–1978.
- (6) Rowe, J. M.; Li, X.; Cassileth, P. A.; et al. *Blood* **2005**, *106*, 3760.

- (7) Damiani, D.; Tiribelli, M.; Raspadori, D.; et al. *Hematol. Oncol.* **2007**, *25* (1), 38–43.
- (8) Shaffer, B. C.; Gillet, J. P.; Patel, C.; et al. *Drug Resist. Updates* **2012**, *15* (1–2), 62–69.
- (9) Xia, C. Q.; Smith, P. G. *Mol. Pharmacol.* **2012**, *82*, 1008–1021.
- (10) de Moraes, A. N.; Maranhão, C. K.; Rauber, G. S.; Claudia Santos-Silva, M. J. *Clin. Lab. Anal.* **2013**, *27*, 62–71.
- (11) Marquez, B.; Van Bambeke, F. *Curr. Drug Targets* **2011**, *12*, 600–20.
- (12) Patel, C.; Stenke, L.; Varma, S.; Lindberg, M. L.; et al. *Cancer* **2013**, *119* (16), 3076–83.
- (13) Sodani, K.; Patel, A.; Anreddy, N.; Singh, S.; et al. *Biochem. Pharmacol.* **2014**, *89*, 52–61.
- (14) Leith, C. P.; Kopecky, K. J.; Chen, I. M.; et al. *Blood* **1999**, *94*, 1086–1099.
- (15) Wu, C. P.; Calcagno, A. M.; Ambudkar, S. V. *Curr. Mol. Pharmacol.* **2008**, *1* (2), 93–105.
- (16) Walter, R. B.; Raden, B. W.; Cronk, M. R.; Bernstein, I. D.; Appelbaum, F. R.; Banker, D. E. *Blood* **2004**, *103* (11), 4276–4284.
- (17) Libby, E.; Hromas, R. *Blood* **2010**, *116* (20), 4037–4038.
- (18) Lourenc, O. J. J.; Maia, R. C.; Scheiner, M. A. M.; Vasconcelos, F. C.; Moreira, M. A. M. *Leuk. Res.* **2008**, *32*, 976–979.
- (19) de Moraes, A. C.; Licínio, M. A.; Zampirolo, J. A.; Liedke, S. C.; et al. *Hematology* **2012**, *17* (2), 59–65.
- (20) Castro, J.; Ribo, M.; Puig, T. *Invest. New Drugs* **2012**, *30*, 880–888.
- (21) Laine, E.; Wolfroth, N.; Enot, D.; Scoazec, M.; et al. *Oncogene* **2013**, *32*, 4331–4342.
- (22) Khamenehfar, A.; Beischlag, T. V.; Russell, P. J.; Ling, M. T. P.; Nelson, C.; Li, P. C. H. *Biomicrofluidics* **2015**, *9* (064104), 1–18.
- (23) Khamenehfar, A.; Wan, C. P. L.; Li, P. C. H.; Letchford, K.; Burt, H. M. *Anal. Bioanal. Chem.* **2014**, *406*, 7071–7083.
- (24) Li, X.; Chen, Y.; Li, P. C. H. *Lab Chip* **2011**, *11* (7), 1378–1384.
- (25) Li, X.; Ling, V.; Li, P. C. H. *Anal. Chem.* **2008**, *80* (11), 4095–4102.
- (26) Li, X.; Huang, J.; Tibbits, G. F.; Li, P. C. H. *Electrophoresis* **2007**, *28* (24), 4723–4733.
- (27) Li, P. C. H. CRC; Taylor and Francis Group: New York, 2006.
- (28) Peng, X. Y.; Li, P. C. H. *Anal. Chem.* **2004**, *76* (18), 5273–5281.
- (29) Jones, T. B. *IEEE Engineering in Medicine and Biology* **2003**, *22* (6), 33–42.
- (30) Braschler, T.; Demierre, N.; Nascimento, E.; et al. *Lab Chip* **2008**, *8*, 280–286.
- (31) Taff, B. M.; Voldman, J. *Anal. Chem.* **2005**, *77* (24), 7976–7983.
- (32) Becker, F. F.; Wang, X. B.; Huang, Y.; Pethig, R.; Vykoukal, J.; Gascoyne, P. R. C. *J. Phys. D: Appl. Phys.* **1994**, *27*, 2659–2662.
- (33) Gascoyne, P. R. C.; Shim, A.; Noshari, J.; Becker, F. F.; Stemke-Hale, K. *Electrophoresis* **2013**, *34*, 1042–1050.
- (34) Raaikimakers, M. H. G. P.; Grouw, E. P. L. M.; Reijden, B. A. V.; Witte, T. J. M.; Jansen, J. H.; Raymakers, R. A. P. *Clin. Cancer Res.* **2006**, *12* (11), 3452–3458.
- (35) Figueiredo-Pontes, L. F.; Pintão, M. C.; Oliveira, L. C. O.; et al. *Cytometry, Part B* **2008**, *74*, 163–168.
- (36) de Greef, G. E.; van Putten, W. L. J.; Boogaerts, M.; Huijgens, P. C.; et al. *Br. J. Haematol.* **2005**, *128* (2), 184–91.
- (37) Sissung, T. M.; Baum, C. E.; Deeken, J.; Price, D. K.; et al. *Clin. Cancer Res.* **2008**, *14* (14), 4543–49.
- (38) Pohl, H. A. *J. Appl. Phys.* **1951**, *22*, 869–871.
- (39) Khamenehfar, A.; Chen, Y.; Hogge, D. E.; Li, P. C. H. *MicroTAS* **2013**, *1*, 380–382.
- (40) Tran, S. L.; Puhar, A.; Ngo-Camus, M.; Ramarao, N. *PLoS One* **2011**, *6* (9), e22876–11.
- (41) Bhattacharjee, S.; Ershov, D.; van der Gucht, J.; Alink, G. M.; Rietjens, I. M. C. M.; et al. *Nanotoxicology* **2013**, *7* (1), 71–84.
- (42) Minko, T.; Pakunlu, R. I.; Wang, Y.; Khandare, J. J.; Saad, M. *Anti-Cancer Agents Med. Chem.* **2006**, *6*, 537–552.
- (43) Pakunlu, R. I.; Cook, T. J.; Minko, T. *Pharm. Res.* **2003**, *20*, 351–359.